The effect of alloying on the properties of $(Nb,Ti)Cr_2$ $C15$ Laves phases

D.J. Thoma [a,*], K.A. Nibur [b], K.C. Chen [b], J.C. Cooley [a], L.B. Dauelsberg [a], W.L. Hults [a], P.G. Kotula [c]

[a] *Los Alamos National Laboratory, Los Alamos, NM 87545, USA*
[b] *California Polytechnic State University, Materials Engineering Department, San Luis Obispo, CA 93407, USA*
[c] *Sandia National Laboratory, Albuquerque, NM, 87185-1405, USA*

Abstract

The effect of composition on the ternary $(NbCr_2-TiCr_2)$ $C15$ phase properties has been investigated, focusing upon the defect structure, elastic properties, and mechanical behavior. The $C15$ phase field is continuous between $NbCr_2-TiCr_2$, with a maximum phase field width of at least 7 at.% solubility. The defect mechanism is governed by anti-site constitutional defects for all alloys. Mechanically, the alloys display a maximum in hardness in the center of the ternary phase field (and a minimum of toughness). The ternary phase field has features that are characteristic of solid-solution strengthening mechanisms. Finally, the elastic properties indicate that the alloys become stiffer in the middle of the ternary phase field. The best compromise of properties occurs furthest from stoichiometry in the ternary phase field at the nominal composition of $Nb_{19}Ti_{19}Cr_{62}$. The relationships between the defect structure, elastic properties, and mechanical response for the C15 phases are discussed using a combination of atomic size arguments and electronic structure analyses. From these relationships, alloy design strategies for $NbCr_2$-based alloys are evaluated.

1. Introduction

Laves phases are the largest class of intermetallics. Over 360 binary phases have been identified, and considering both binary and ternary systems, over 900 phases exist [1]. Despite their abundance, the limitation of Laves phases for engineering applications results from the general observation that they display brittle behavior. Fabrication and utilization are limited by the inability to retain structural integrity. However, Laves phases, as a class of material, display encouraging high-temperature properties. Most notably, the alloys retain over 85% of their strength at half of their homologous melting temperature [2], and brittle to ductile transition temperatures occur at $0.65T_m$ [3]. Therefore, the challenge is to utilize the overwhelming abundance of Laves phases to tailor alloying opportunities for optimized mechanical properties. This requires a fundamental approach to alloying strategies and interpretation of the resultant properties.

Less than 25% of the known binary Laves phases exhibit a measurable range of solubility [1]. The $C15$ phases that do display solubility are those that exist between elemental metallic radii ratios (R_A/R_B) of 1.1 and 1.35. In the AB_2 structure, the ideal size ratio of the atom sizes in the ordered structure is $\sqrt{(3/2)} \approx 1.225$ as defined by near neighbor distances of the A and B atoms. Since Laves phases are predominantly metallic in bonding nature and largely governed by geometric space filling principles [4], solubility is related to the ability of A and B atoms to expand or contract so that the ideal ratio is approached [5]. Therefore, geometric rules have been developed to predict alloying behavior in Laves phases [1]. From this approach, it has been proposed that a simple and effective strategy for a broadened ternary alloy phase field would require $R_A > R_C > R_B$, where C is the ternary addition to the AB_2 intermetallic.

---

* Corresponding author.

Among the Laves phases, $NbCr_2$ shows interesting promise for high-temperature structural applications. For example, $NbCr_2$ has a high melting point (1730 °C) [6], reasonable density (7.7 g/cm^{-3}), high strength [7], excellent creep behavior [8], and reasonable oxidation resistance (below 1000 °C). However, the material is brittle and requires modification to be a viable engineering material. Based upon the simple geometric principles, Ti ($R_{Nb} > R_{Ti} > R_{Cr}$) would be an appropriate alloying addition to broaden the ternary phase field and define the property response as a function of composition. Since Ti is only slightly smaller than Nb, $C15$ $NbCr_2$ ($R_{Nb}/R_{Cr} = 1.15$) and $TiCr_2$ ($R_{Ti}/R_{Cr} = 1.14$) display a continuous phase field [9]. In addition, the $C15$ phase field displays a 7at.% solubility range towards the Cr-lean side in the room temperature ternary isotherm. The goal of this study is to interpret the influence of alloying on properties in the $NbCr_2$-$TiCr_2$ $C15$ Laves phase field.

2. Experimental procedure

Elemental Nb, Cr, and Ti with nominal purities of 99.9at.%, 99.99at.%, and 99.99at.% respectively, were arc-cast into eight different 30 g ingots with varying nomimal compositions (Table 1). The ingots were arc-cast on a water-cooled copper hearth. The arc-melting chamber was evacuated to 0.5 Pa and purged at least three times with high purity argon. Titanium buttons were melted as oxygen getters before each ingot melting. The ingots were inverted and melted ten times to ensure chemical uniformity.

Heat-treatments of the ingots consisted of 48 h at 1300 °C, 100 h at 1400 °C, and 100 h at 1200 °C, followed by a 1 °C/min. furnace cool. The first step homogenizes the ingots before any melting of segregated regions occurred. The 1400 °C step provides more complete chemical homogeneity, and the 1200 °C treatment is used to homogenize below the expected polytype transformation ($C14-C15$). All ingots were wrapped first with Nb foil and then Ti foil. The furnace system

was evacuated (to 0.5 Pa) and purged three times before heating, with the heat-treatment occurring in a flowing environment of high-purity argon. A boat of Ti chips was placed in the hot-zone of the furnace upstream from the sample as an oxygen getter for the incoming argon stream.

The compositions of the ingots were evaluated using electron microprobe analyses. Standard-based analyses were used, with examinations performed at an accelerating voltage of 15 kV. Lattice parameters were determined using Cu $K\alpha$ radiation. Silicon standards were mixed with the samples and cell refinement analyses were used to determine the lattice parameters.

The mechanical properties were surveyed using microhardness indentation. A Vickers hardness indenter was used with a 500 g load and a dwell time of 15 s. Twenty measurements were made on each sample. Furthermore, toughness was evaluated by examining the crack lengths made during indentation. Scanning electron microscopy was used to measure the crack lengths, and the toughness was determined using the equation [10]:

$$K = 0.016 \left(\frac{E}{H} \right)^{1/2} \left(\frac{P}{c^{3/2}} \right) \quad (1)$$

In the equation, E is the Young's modulus, H is the hardness, P is the applied load, and c is the average crack length.

Resonant ultrasound spectroscopy (RUS) [11,12] was used to study the room temperature elastic properties of the polycrystalline alloys. The specimens were cut into rectangular parallelpipeds (roughly $2 \times 3 \times 4$ mm) and ground to final finish using 800 grit SiC paper. The mass-densities of the specimens were determined from their dimensions and masses. For this study, 15–30 resonant peaks from 0.2 MHz–1.5 MHz were used for each sample to determine the elastic constants. In the measurement, the samples were assumed to be isotropic and only two elastic constants, c_{11} and c_{44}, were fitted in the RUS procedures. In this case, the bulk modulus B, shear modulus G, Young's modulus E, and Poisson's ratio v, can be obtained through

Table 1
List of nominal compositions, actual compositions (determined from microprobe studies) and lattice parameters of the alloys used

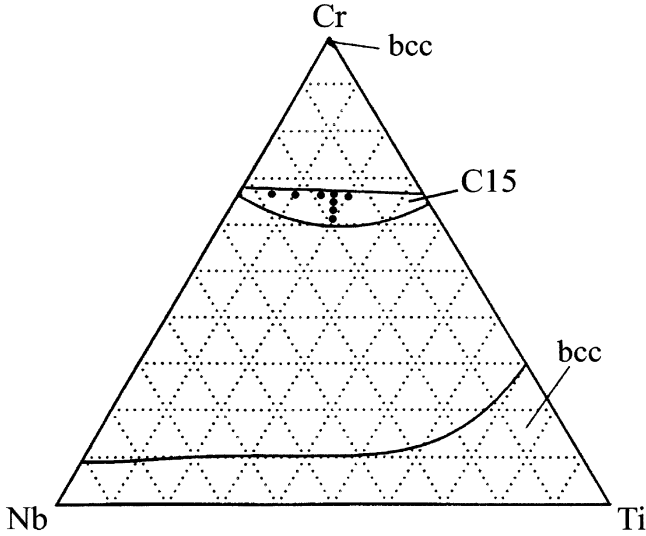| Sample number	Nominal composition (at.%)			Measured composition (at.%)			Lattice parameter
	Nb	Ti	Cr	Nb	Ti	Cr	(Angstroms)
1	28	5	67	29.8	4.0	66.2	6.9778 ± 0.0001
2	23	10	67	24.8	9.2	66.0	6.9675 ± 0.0002
3	18	15	67	19.8	14.0	66.2	6.9583 ± 0.0001
4	13	20	67	14.5	19.5	66.0	6.9495 ± 0.0002
5	16	16	68	18.4	15.6	66.0	6.9556 ± 0.0001
6	17	17	66	18.1	16.1	65.8	6.9594 ± 0.0001
7	18	18	64	19.4	16.9	63.7	6.9717 ± 0.0001
8	19	19	62	20.1	17.3	62.6	6.9882 ± 0.0001

Fig. 1. The ternary phase diagram for Nb-Cr-Ti [9]. Shown in the NbCr₂-TiCr₂ $C15$ phase field are the compositions of the alloys investigated in this study. The horizontal row of alloys are along the $(Nb_{33-x}Ti_x)Cr_{67}$ isopleth, and the vertical row of alloys are along the $(Nb_xTi_x)Cr_{67-2x}$ constant Nb/Ti plethal section.
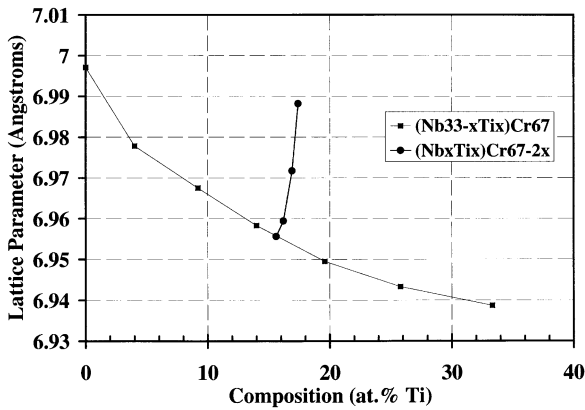

Fig. 2. The lattice parameters for the $C15$ Laves phases. The alloys along the $(Nb_{33-x}Ti_x)Cr_{67}$ isopleth display a negative deviation from a linear rule of mixtures. The alloys along the $(Nb_xTi_x)Cr_{67-2x}$ constant Nb/Ti plethal section increase rapidly with increasing Ti content. The data for NbCr₂ [6], TiCr₂ [13], and Nb₉.₅Ti₂₆Cr₆₅.₅ [14] were taken from the literature.

$$B = \frac{1}{3}(3c_{11} - 4c_{44})$$

$$G = c_{44}$$

$$E = \frac{c_{44}(3c_{11} - 4c_{44})}{c_{11} - c_{44}}$$

$$v = \frac{1}{2}\frac{c_{11} - 2c_{44}}{c_{11} - c_{44}} \tag{2a-2d}$$

The overall r.m.s errors for the measured RUS peaks were less than 0.5%, indicating an acceptable fit to the experimental elastic moduli.

3. Results

3.1. Compositions and lattice parameters

A ternary isotherm of the Nb-Cr-Ti phase diagram (at 950 °C) is shown in Fig. 1 [9]. The nominal compositions of the alloys are displayed in the $C15$ phase field, illustrating the isoplethal set of alloys $[(Nb_{33-x}Ti_x)Cr_{67}]$ and the constant Nb/Ti plethal alloys $[(Nb_xTi_x)Cr_{67-2x}]$. Based upon the phase field, the primary constitutional defect would be expected to be a substitution of Nb and Ti on A sub-lattice sites.

The experimental compositions of the samples are compared to the nominal compositions in Table 1. In all but one sample, the Cr and Ti content was slightly less than the intended values, but overall, the compositional control was satisfactory. The lattice parameters are also given in Table 1. When the lattice parameters are plotted against these compositions, systematic trends are evident (Fig. 2). The lattice parameters of the samples along the chromium isopleth $\{(Nb_{33-x}Ti_x)Cr_{67}\}$ illustrate a slight negative deviation between NbCr₂ and TiCr₂. The values for NbCr₂ [6] and TiCr₂ [13] were taken from the literature as was the data for Nb₉.₅Ti₂₆Cr₆₄.₅ [14]. The negative deviation from an ideal rule of mixtures suggests tighter binding when Nb and Ti occupy the A sub-lattice as compared to the binary phases.

The lattice parameters of the samples along the constant Nb/Ti plethal section $[(Nb_xTi_x)Cr_{67-2x}]$ increase rapidly as the Cr content decreases (Ti content increases). This suggests that the operative defect mechanism is Nb and/or Ti substituting onto the B sub-lattice. In fact, this result is consistent with a study that used Atom Location by Channeling Enhanced MIcroanlaysis (ALCHEMI) [15]. This study suggested that, on the Cr-lean side of the constant Nb/Ti plethal section, Ti preferentially substitutes onto the B sub-lattice (as opposed to Nb). On the A sub-lattice sites, only Nb and Ti occupy the sites.

3.2. Hardness properties

The hardness data along the Cr isopleth (Fig. 3) and the constant Nb/Ti plethal section (Fig. 4) indicates subtle increases in hardness as a function of increasing Ti content. As titanium substitutes for Nb, the hardness increases slightly towards the middle of the phase field. From the middle of the NbCr₂-TiCr₂ isopleth, substitution of Ti onto the B sub-lattice further increases the hardness. The trend suggests that the further away it is away from stoichiometry, the harder the $C15$ phase becomes.

In contrast to the hardness data, the toughness data along the isoplethal section are relatively constant (Fig. 5). However, along the constant Nb/Ti plethal section,

the toughness appears to increase slightly with increasing Ti content (decreasing Cr content) (Fig. 6). Interestingly, the standard deviation increases substantially. Nonetheless, the monolithic $C15$ phase becomes
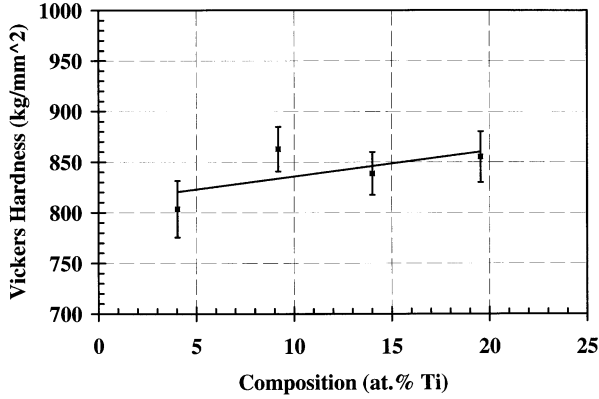

Fig. 3. The Vickers hardness data as a function of Ti content along the $(Nb_{33-x}Ti_x)Cr_{67}$ isopleth.
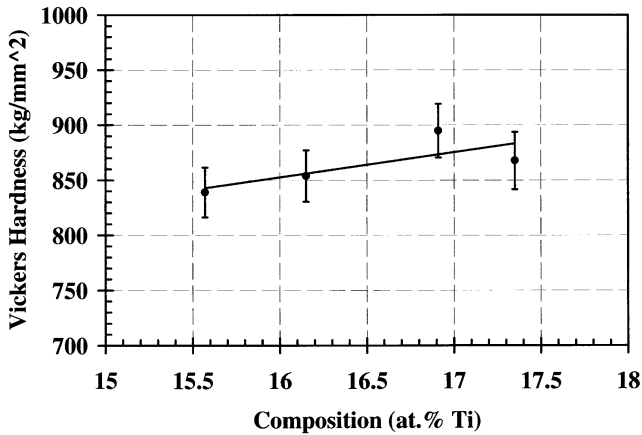

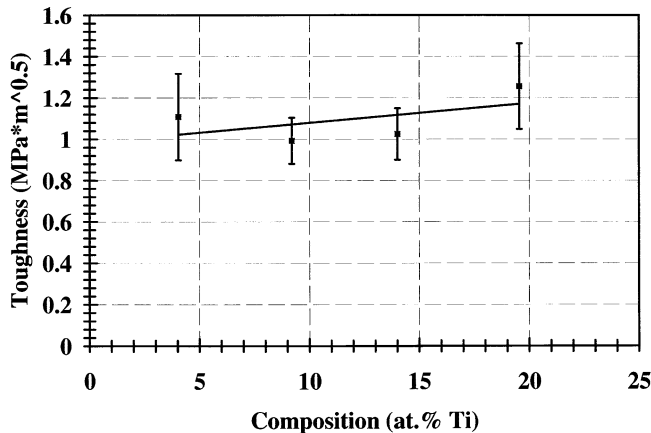Fig. 4. The Vickers hardness data as a function of Ti content along the $(Nb_xTi_x)Cr_{67-2x}$ constant Nb/Ti plethal section.

Fig. 5. The toughness data (determined from crack lengths developed during indentation) along the $(Nb_{33-x}Ti_x)Cr_{67}$ isopleth.
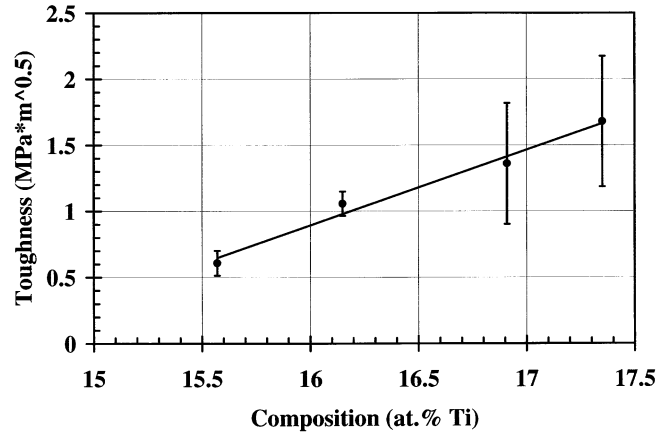

Fig. 6. The toughness data (determined from crack lengths developed during indentation) along the $(Nb_xTi_x)Cr_{67-2x}$ constant Nb/Ti plethal section.

slightly harder as anti-site substitution on the A and B sites is increased.

3.3. Elastic properties

The elastic properties of the alloys are given in Table 2 along with the values for $NbCr_2$ [16] and $TiCr_2$ [17]. The data for sample #1 could not be evaluated because of the inability to obtain a good fit of the data. It is possible that microcracks deteriorated the ability to determine elastic constants with reasonable fits. In addition, the data for sample #6 may be experiencing the same difficulties. Nonetheless, the properties, in general, are within approximately 10% of each other, illustrating that the elastic properties do not change remarkably within the ternary $C15$ phase field. The Youngs's modulus is ~ 210 GPa for all of the alloys, the Poisson's ratio is around 0.3, and the shear modulus is approximately 80 GPa. However, subtle trends do exist. The most notable are the shear and Young's modulii. Along the Cr isopleth, the shear modulus display a positive deviation from a rule of mixtures, whereas the Young's modulus roughly follows a rule of mixtures (Fig. 7). Along the constant Nb/Ti plethal section, the elastic properties systematically decrease as the Ti content increases (Cr content decreases) (Fig. 8). Thus, as anti-site substitution increases on the B sublattice, the alloys become less stiff.

4. Discussion

4.1. Phase stability and defect structure

The phase diagram and lattice parameters, coupled with ALCHEMI results, clearly indicate that Ti primarily substitutes for Nb in the $C15$ phase field of the Nb-Cr-Ti ternary system. This result is expected since

Table 2
List of elastic properties for the alloys studied

Sample number	Nominal composition Nb-Ti-Cr (at.%)	Young's modulus, E (GPa)	Shear modulus, G (GPa)	Bulk modulus, B (GPa)	Poisson's ratio, v
NbCr₂[a]		214.1	79.6	229.4	0.34
2	23–10–67	212.4	82.0	172.9	0.30
3	18–15–67	212.9	83.3	159.8	0.28
4	13–20–67	210.2	82.1	159.4	0.28
TiCr₂[b]		203.9	78.8	165.5	0.29
5	16–16–68	219.6	84.6	180.8	0.30
6	17–17–66	219.0	83.1	200.0	0.32
7	18–18–64	214.8	83.0	174.0	0.29
8	19–19–62	213.0	82.6	168.7	0.29

[a] From [14].
[b] From [15].

the atomic radii of metallic Nb ($R = 1.468$) and Ti ($R = 1.462$) are similar. The stability and adundance of Laves phases have historically been attributed to geometric space filling principles, and the results of this study are certainly consistent with this view. However, from size arguments alone, it is easier to conceptualize a broader phase field on the Cr-rich side stoichiometry as contrasted to the experimental observation of enhanced solubility on the Cr-lean side of the Nb/Ti plethal section. For example, assuming a hard-ball model, a smaller Cr atom ($R = 1.282$) can be 'packed' into an A sub-lattice more easily than a (Nb,Ti) atom on a B sub-lattice site. This contradiction to a size rule can be interpreted through a consideration of the electronic structure. First-principles electronic and total energy calculations show that the Fermi energy of $C15$ NbCr₂ reaches such a level that substantial amount of antibonding electronic states of the system are occupied [18,19]. Since this is not an energetically favorable condition, it is possible that alloying methodologies that lower the valence electron contributions should be favored [20]. Titanium has a lower valence state than niobium, and niobium has a lower valence state than chromium. Therefore, from an electronic structure argument, Ti or Nb occupancy of Cr atom sites may reduce the number of filled anti-bonding states. Accordingly, the Fermi level will be located at a lower density of states. The more energetically favorable electronic structure may account for solubility on the Cr-lean side of stoichiometry, despite the fact that the Nb or Ti atom is larger than the Cr atom. In fact, this electronic argument may provide insight into the observed result from ALCHEMI experiments that Ti is preferential to Nb in substituting onto the B sub-lattice. Since Ti has a lower valence than Nb, it would be a more efficient substitution to provide a more energetically favorable electronic structure. Details of the TiCr₂ electronic structure would substantiate this hypothesis.
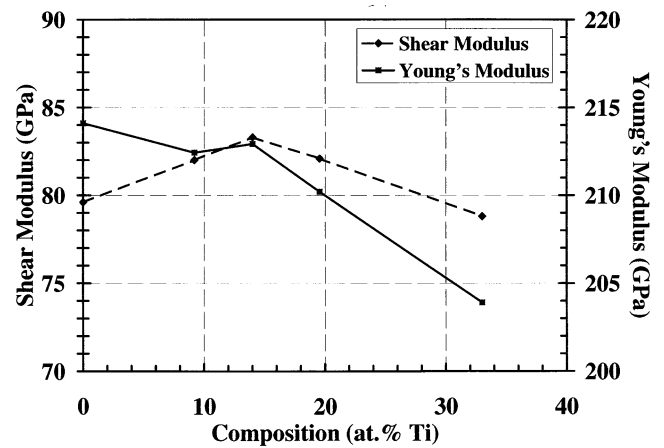

Fig. 7. The shear and Young's moduli for alloys along the ($Nb_{33-x}Ti_x$)Cr_{67} isopleth. The data for NbCr₂ is from [16], and the data for TiCr₂ is from [17].
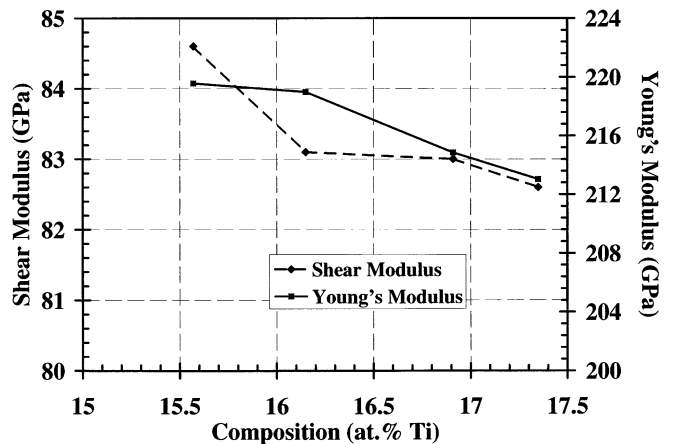

Fig. 8. The shear and Young's moduli for alloys along the (Nb_xTi_x)Cr_{67-2x} constant Nb/Ti plethal section.

4.2. Mechanical behavior

Due to the specific arrangement of atoms, deformation involving simple planar slip is unlikely and a 'synchros-hear' or 'zonal slip' mechanism involving cooperative movement between planes of atoms may be required in Laves phases [21–23]. The mechanism of synchroshear is graphically illustrated in Fig. 9. The deformable layer in the structure has been proposed to consist of the $\alpha c \beta$ 'sandwich'. The smaller B atoms shear by $1/6[-211]$ while synchronously, the larger A atoms shear by $1/6[-1-12]$. In other words, the smaller atoms move from the illustrated c-site to the b-site while the larger atoms move from the β-site to the γ-site. The synchroshear process has been used to interpret slip, twinning, stacking faults, and phase transformations in Laves phases.

From the interpretation of synchroshear, an effective alloying addition would consist of a smaller atom onto the A sub-lattice site. This has been postulated to enhance shear deformation in $C15$ structures [24], thus making Ti an attractive addition for Nb to provide more deformability in $NbCr_2$. However, the hardness increases and the toughness does not increase substantially as Ti substitutes for Nb. These results may be correlated to the lattice parameters, where a negative deviation from a rule of mixtures exist. The lattice actually contracts, providing higher packing in the deformable $\alpha c \beta$ sequence than expected from a hard sphere viewpoint. The tighter binding may translate to less slip during deformation. The tighter binding is also reflected in the higher shear modulus (a positive deviation from a rule of mixtures) with respect to the terminal binary phases.

The size arguments on deformation have been used for B site occupancy [19]. In $Nb(Cr,V)_2$, V was found to preferentially subsititute on the B-sublattice, and since $R_{Cr} < R_V$, the packing density of atoms within the
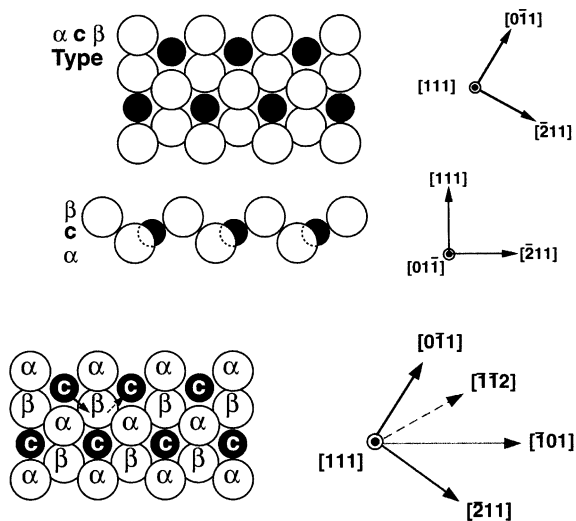
deformable $\alpha c \beta$ sandwich would increase, therefore 'locking' the deformation mechanism. Specifically, for $Nb_{33}Cr_{42}V_{25}$ the lattice parameter changed only 1% as compared to $NbCr_2$, but the elemental vanadium atomic radius was 5% larger than chromium. This resulted in higher strength, higher shear modulus, lower fracture toughness, and a higher brittle to ductile transition temperature. However, with Ti substitution onto the Cr lattice, this trend is not evident. Elemental Ti is 14% larger than Cr, and the lattice parameter only changes 0.5% between the nominal compositions of $Nb_{16}Ti_{16}Cr_{68}$ and $Nb_{19}Ti_{19}Cr_{62}$. Thus, making the same argument with V substitution, the deformation mechanism should be even more restricted than with the case of vanadium substitutions onto Cr sites. The data illustrate that the alloys along the constant Nb/Ti plethal section become harder, but the elastic moduli decrease and the toughness increase. This is the most intriguing aspect of this study, and will be the focus of future studies.

4.3. Elastic properties

Overall, the elastic properties of the $(Nb,Ti)Cr_2$ Laves phases are interesting as compared to other intermetallic systems. The shear moduli are comparable to nickel aluminides and higher than titanium aluminides, and much lower than transition metal silicides. The shear modulus values for the ternary alloys suggest a maximum in the middle of the phase field, and a decreasing trend as the alloys become Cr-lean. All ternary alloys had a slightly higher shear modulus as compared to the binary $C15$ phases.

The Poisson's ratios of the alloys were all approximately 0.3. This number reflects the volume change during uniaxial deformation. If v is $1/2$, no volume change occurs. Furthermore, the Poisson's ratio provides information about the directionality of bonding forces. A Poisson's ration of $v = 0.5$ is an upper limit that corresponds to infinite elastic isotropy, while a value of 0.25 is a lower limit for central-force polycrystals. The Poisson's ratios in this study are higher than aluminides and silicides, suggesting less-directional interatomic forces than those of other high-temperature structural intermetallics. However, all values were lower than the measured values of $NbCr_2$, suggesting that increased bonding directionality may be occurring with Ti additions.

4.4. Alloying strategies

The methodology to choose alloying elements based upon geometric considerations is an effective strategy for a first level attempt in selecting elements for property modification. For Laves phases, the simple requirement that $R_A > R_C > R_B$ (where C is the ternary alloying element to the AB_2 Laves phase) has proven to

Fig. 9. The deformable $\alpha c \beta$ stacking sandwich in the $C15$ structure (redrawn from [ ]).

be consistent for large extensions of the ternary phase field. These geometric considerations are founded upon more detailed investigations on the occurrence of solubility in Laves phases. The alloying selections can be further refined with a fundamental understanding of the electronic structure, with valence states being a useful guide for site-occupancy. Of course, this requires that reasonable estimates of the Fermi level energy positions with respect to the total density of states are made. In all of these estimates, it is a reasonable assumption that only anti-site substitution (as opposed to constitutional vacancies) occurs in Laves phases since contrary information is almost non-existent.

With useful tactics on how to alloy the Laves phase, specific property modifications can be addressed. To address deformability in $C15$ phases, the assumption that synchroshear is the operative defect mechanism is a guiding principle. Since deformation occurs in the $\alpha c\beta$ stacking sandwich, reduction of the activation barriers and Burger's vectors is an appropriate goal, and this may be most easily obtained by substituting a smaller C atom onto an A site. From a hard sphere concept, this would facilitate synchroshear. However, although Ti is smaller than Nb, the lattice collapses with Ti substitutions onto the Nb sites, and atom binding appears to be tighter and slightly more directional. As a result, significant enhancement of the synchroshear process does not occur along the isoplethal section. A careful balance between site occupancy and packing efficiency is required and apparently is not achieved along the isopleth. Other features such as stacking fault energy need more investigation to elucidate mechanical response, and efforts are underway to achieve this goal.

The most useful alloying result in $NbCr_2$-$TiCr_2$ alloys occurs away from Cr stoichiomety. As alloying in the ternary phase field is maximized (i.e. substitution of Ti on both A and B sites), the alloys display higher hardness and the increased toughness. Moreover, the elastic moduli gradually decrease with respect to deviations from stoichiometry of the isoplethal alloys. This is an interesting observation in that a similar event may be occurring in $HfV_2 + Nb$ [24], with Nb substituting preferentially on Hf sites, but also on V sites [15], resulting in plastic deformation at room temperature. This raises the notion that deformability may be linked to site substitutions on both sites (not just the A site) with a corresponding decrease in the order parameter. With this information, the best choice of an alloy to produce a dual-phase microstructure (bcc/$C15$ phases) would be alloys comprised of the $Nb_{19}Ti_{19}Cr_{62}$ (maximum limit of the phase field) and the (Nb,Ti) base bcc solid solution. In fact, recent studies have shown that these alloys have encouraging combinations of high-temperature strength [7] and room temperature toughness [25]. Varying volume fractions of the Laves phase with respect to a bcc (Nb,Ti) base matrix are currently being explored to expand upon this possiblity.

5. Conclusions

The effect of alloying in the $NbCr_2$-$TiCr_2$ $C15$ phase field has been explored. The defect mechanisms and phase stability have been examined, and the resulting mechanical behavior and elastic properties were investigated. Five conclusions can be drawn from this work:

1. The ternary phase field is continuous between $NbCr_2$ and $TiCr_2$, with a 7% phase field extension to Cr-lean alloys. In all cases, the defect mechanism appears to be anti-site substitution, and the alloying can be interpreted based upon geometric space filling principles coupled with electronic structure arguments.
2. The lattice parameters along the $(Nb_{33-x}Ti_x)Cr_{67}$ isoplethal section show a negative deviation from a linear rule of mixtures (suggesting tighter binding than the binary phases), and lattice parameters along the constant Nb/Ti plethal section $[(Nb_xTi_x)Cr_{67-2x}]$ increase rapidly, consistent with anti-site substitutions.
3. Titanium additions to $NbCr_2$ increase the hardness along both the Cr isoplethal section and the constant Nb/Ti plethal section. The toughness increased only along the constant Nb/Ti plethal section.
4. With Ti additions, the elastic properties all increase with respect to $NbCr_2$, with all Poisson's ratios being slightly less than $NbCr_2$ (0.3 vs 0.34). The shear moduli along the Cr isoplethal section showed a positive deviation with respect to a linear rule of mixtures between $NbCr_2$ and $TiCr_2$, correlating with the increased hardness and the negative deviation of the lattice parameters (with respect to a rule of mixtures).
5. The elastic moduli gradually decreased along the constant Nb/Ti plethal section.

All of these results suggest that the optimized combination of properties exist in the $C15$ phase that was furthest from $NbCr_2$ stoichiometry ($Nb_{19}Cr_{19}Ti_{62}$).

References

[1] D.J. Thoma, J.H. Perepezko, J. Alloys Compds. 224 (1995) 330.

[2] R.L. Fleischer, MRS Symp. Proc. 133 (1989) 305.

[3] D.J. Thoma, F. Chu, P. Peralta, P.G. Kotula, K.C. Chen, T.E. Mitchell, Mat. Sci. & Eng. A. 239–240 (1997) 251.

[4] F. Laves, Theory of Alloy Phases, ASM, Cleveland, OH, 1956, p. 123.

[5] A.E. Dwight, Trans. ASM 53 (1961) 479.

[6] D.J. Thoma, J.H. Perepezko, Mater. Sci. & Eng. A. 156 (1992) 97.

[7] K.C. Chen, P.G. Kotula, C.M. Cady, M.E. Mauro, D.J. Thoma, MRS Symp. Proc. 552 (1999) KK7.4.1.

[8] D.L. Anton, D.M. Shah, MRS Symp. Proc. 213 (1991) 733.

[9] D.J. Thoma, J.H. Perepezko, in: J.E. Morral, R.S. Schiffman, S.M. Merchant (Eds.), Experimental Methods of Phase Diagram Determination, TMS, Warrendale, PA, 1993, p. 43.

[10] G.R. Anstis, P. Chantyikul, B.R. Lawn, D.B. Marshall, J. Amer. Cera. Soc. 64 (1981) 533.

[11] A. Migliori, et al., Physica B. 183 (1993) 1.

[12] F. Chu, M. Lei, A. Migliori, S.P. Chen, T.E. Mitchell, Phil. Mag. B. 70 (1994) 867.

[13] K.C. Chen, S.M. Allen, J.D. Livingston, Mater. Sci. Eng. A242 (1998) 163.

[14] D.J. Thoma, J.H. Perepezko, Mater. Sci. Forum 179–181 (1995) 769.

[15] P.G. Kotula, I.M. Anderson, F. Chu, D.J. Thoma, J. Bentley, T.E. Mitchell, MRS Symp. Proc. 460 (1997) 617.

[16] F. Chu, Y. He, D.J. Thoma, T.E. Mitchell, Scripta Metall. et Mater. 33 # 8 (1995) 1295.

[17] Chu F., Thoma D.J. unpublished data.

[18] A. Ormeci, F. Chu, J.M. Wills, T.E. Mitchell, R.C. Albers, D.J. Thoma, S.P. Chen, Phys. Rev. B. 54 (1996) 12753.

[19] F. Chu, D.J. Thoma, P.G. Kotula, S. Gerstl, T.E. Mitchell, I.M. Anderson, J. Bentley, Acta Mater. 46 (1998) 1759.

[20] A. Ormeci, S.P. Chen, J.M. Wills, R.C. Albers, MRS Symp. Proc. 552 (1999) KK8.30.1.

[21] C.W. Allen, K.C. Liao, A.E. Miller, J. Less-Common Metals 52 (1977) 109.

[22] J.D. Livingston, Phys. Stat. Sol. (a) 131 (1992) 415.

[23] F. Chu, D.P. Pope, Mater. Sci. & Eng. A. 170 (1993) 39.

[24] F. Chu, D.P. Pope, MRS Symp. Proc. 288 (1993) 561.

[25] D.L. Davidson, K.S. Chan, Scripta Mater. 38 (# 7) (1998) 1155.